Mutual Interdependence of Spin Crossover and Metal−Metal Bond Formation in $M_2Cl_9^{3-}$ (M = Fe, Ru, Os)

Timothy Lovell,[†,‡] Robert Stranger,*[,†] and John E. McGrady*[,§]

Department of Chemistry, The Faculties, The Australian National University, Canberra, ACT 0200, Australia, and Department of Chemistry, The University of York, Heslington, York, YO10 5DD, U.K.

Received May 1, 2000

Broken-symmetry density functional theory is used to examine the coupling between metal ions in the face-shared bioctahedral complexes $M_2Cl_9^{3-}$, M = Fe, Ru, Os. In the ruthenium and osmium systems, the metal ions have low-spin configurations, and strong coupling results in the formation of a metal−metal σ bond. In contrast, the iron system contains two weakly coupled high-spin Fe^{III} centers, the different behavior being due to the high spin-polarization energy in the smaller Fe atom. At Fe−Fe separations shorter than 2.4 Å, however, an abrupt transition occurs and the ground state becomes very similar to that for the heavier congeners (i.e., strongly coupled low-spin Fe^{III}). The intrinsic link between high-spin/low-spin transitions on the individual metal centers and the onset of metal−metal bond formation is traced to the spin-polarization energy, which plays a central role in both processes.

Introduction

In a series of recent publications we have examined the factors that determine the strength of interaction between metal ions in face-shared bimetallic clusters, $M_2Cl_9^{z-}$(Figure 1).[1] In the presence of bridging ligands, the complex does not depend on covalent metal−metal bonding for its stability, and as a consequence, the strength of the interactions between the metal ions can vary widely, from the multiple covalent metal−metal bonds observed in species such as $W_2Cl_9^{3-}$ to the weak antiferromagnetic coupling present in its chromium congener.[1−3] The strength of the interaction is determined by a competition between two factors: (i) the overlap between the orbitals on opposite metal centers and (ii) the exchange (or spin-polarization) energy associated with the presence of unpaired electron density.[1b,4] In complexes of the second and third transition series, the diffuse 4d and 5d orbitals ensure that the overlap is large, typically giving rise to strong covalent metal−metal bonds. In their isoelectronic first-row counterparts, in contrast, the high spin-polarization energy dominates, giving localized electron distributions and weak antiferromagnetic coupling. Reference 1 has dealt exclusively with complexes where electrons occupy only the orbitals derived from the t_{2g} subset of the parent octahedron. The purpose of this paper is to extend this theoretical framework to include systems where occupation of the metal−ligand antibonding e_g manifold is also possible. In such circumstances, transitions between low- and high-spin configurations on the individual metal ions add a further degree of complexity to the problem.

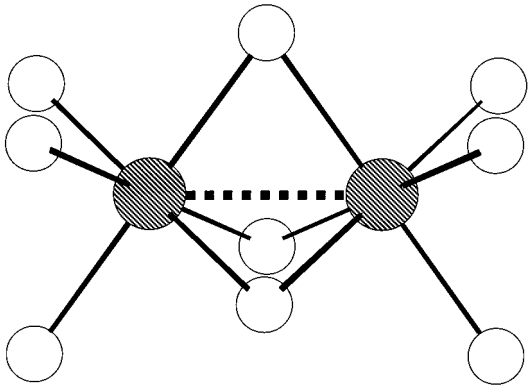

Figure 1. Structure of a face-shared bioctahedral complex, $M_2Cl_9^{z-}$.

In addition to the intrinsic interest from the point of view of electronic structure, the results reported herein may also bear some relevance to recent developments in the field of bioinorganic chemistry. Iron-containing clusters are a common structural motif at the active site of metalloenzymes,[5] well known examples including iron−sulfur cubanes[6,7] and the family of non-heme iron proteins.[8] In their resting oxidation states, distances between the metal centers are typically large and

[†] The Australian National University.

[‡] Current address: Department of Molecular Biology, The Scripps Research Institute, La Jolla, CA 92037.

[§] The University of York.

(1) (a) Lovell, T.; McGrady, J. E.; Stranger, R.; Macgregor, S. A. *Inorg. Chem.* **1996**, *35*, 3079. (b) McGrady, J. E.; Stranger, R.; Lovell, T. *Inorg. Chem.* **1997**, *36*, 3242. (c) McGrady, J. E.; Stranger, R.; Lovell, T. *J. Phys. Chem. A* **1997**, *101*, 6265. (d) McGrady, J. E.; Stranger, R.; Lovell, T. *Inorg. Chem.* **1998**, *37*, 3802 (e) Stranger, R.; McGrady, J. E.; Lovell, T. *Inorg. Chem.* **1998**, *37*, 6795. (f) Stranger, R.; Lovell, T.; McGrady, J. E. *Inorg. Chem.* **1999**, *38*, 5510. (g) McGrady, J. E. *J. Chem. Soc., Dalton Trans.* **1999**, 1393.

(2) (a) Dunbar, K. R.; Pence, L. E. *Acta Crystallogr.* **1991**, *C47*, 23. (b) Watson, W. H., Jr.; Waser, J. *Acta Crystallogr.* **1958**, *11*, 689. (c) Stranger, R.; Grey, I. E.; Madsen, I. C.; Smith, P. W. *J. Solid State Chem.* **1987**, *69*, 162.

(3) (a) Saillant, R.; Wentworth, R. A. D. *Inorg. Chem.* **1968**, *7*, 1606. (b) Grey, I. E.; Smith, P. W. *Aust. J. Chem.* **1971**, *24*, 73.

(4) Poli, R.; Mui, H. D. *Inorg. Chem.* **1991**, *30*, 65.

(5) Holm, R. H.; Kennepohl, P.; Solomon, E. I. *Chem. Rev.* **1996**, *96*, 2239.

(6) Noodleman, L.; Case, D. A. *Adv. Inorg. Chem.* **1992**, *38*, 423.

(7) Howard, J. B.; Rees, D. C. *Chem. Rev.* **1996**, *96*, 2965.

(8) Solomon, E. I.; Brunold, T. C.; Davis, M. I.; Kemsley, J. N.; Lee, S.-K.; Lehnert, N.; Neese, F.; Skulan, A. J.; Yang, Y.-S.; Zhou, J. *Chem. Rev.* **2000**, *100*, 235.

10.1021/ic0004737 CCC: $20.00
Published on Web 12/08/2000

interactions weak. Recent experimental results, however, suggest that Fe−Fe interactions may be significantly enhanced in highly reduced forms of the Fe protein in the nitrogenase enzyme.[9] Reduction of an iron−sulfur cubane to the all-ferrous level has been shown to induce a significant geometric distortion in the 4Fe−4S core, resulting in an Fe−Fe distance much shorter than that observed in other model iron−sulfur clusters and resembling the short Fe−Fe distances noted in the all-ferrous P^N state of the nitrogenase P clusters.[10] Short Fe−Fe separations have also been observed in high-valent diiron intermediates involved in the catalytic cycles of methane monooxygenase[11] and ribonucleotide reductase,[12] as well as a peroxo-bridged diferric intermediate in the biomineralization pathway in ferritin.[13] The presence of metal−metal separations as small as 2.5 Å in these reactive intermediates may be indicative of a functional role for metal−metal interactions in controlling electron transfer between metal and ligand.[14]

Computational Details

All calculations described in this work were performed on either Sun UltraSparc 140/170 workstations or Linux-Pentium II 333/400 MHz computers using the Amsterdam density functional (ADF) program, version 2.3, developed by Baerends et al.[15] The local density approximation[16] to the exchange potential was used, along with the correlation potential of Vosko, Wilk, and Nusair.[17] The LDA was used throughout, as previous work has shown that the incorporation of nonlocal corrections to the exchange−correlation potential leads to generally poorer agreement with experiment, particularly in relation to metal−metal distances.[1c] A double-ξ Slater-type orbital basis set extended with a single d-type polarization function was used to describe Cl, while all metals were modeled with a triple-ξ basis. Electrons in orbitals up to and including 2p {Cl}, 3p {Fe}, 4p {Ru}, and 5p {Os} were considered to be part of the core and treated in accordance with the frozen core approximation. Geometries were fully optimized using the algorithm of Versluis and Ziegler.[18] In the broken-symmetry calculations, all symmetry elements connecting the two centers were removed, resulting in overall C_{3v} point symmetry, and an asymmetry in the initial spin densities was introduced using the modifystartpotential key. Potential energy curves were obtained by freezing the metal−metal distance and optimizing all other independent structural parameters. No attempt was made to use approximate spin projection techniques to obtain the energy of the singlet ground state, as we have illustrated previously that where such a procedure is valid the singlet state lies very close to the broken-symmetry curve.[1c]

Results and Discussion

Spin Crossover in Monomeric Complexes, MCl_6^{3-}. For octahedral d^5 complexes, both the low-spin $^2T_{2g}$ and high-spin $^6A_{1g}$ states are well represented by single-determinant configurations, $t_{2g}^{3/2}e_g^{0/0}$ and $t_{2g}^{3/0}e_g^{2/0}$, respectively (configurations, summarized in Table 1, are denoted $\Gamma^{\alpha/\beta}$, where Γ is the symmetry label of the orbital and α and β are the occupations of the spin-up and spin-down components, respectively). The energies and optimized M−Cl bond lengths for the high- and low-spin states of $FeCl_6^{3-}$, $RuCl_6^{3-}$, and $OsCl_6^{3-}$ are summarized in Table 2. The relative stabilities of the two configurations are fully in accord with experimental findings, showing a clear preference for high spin in the iron complex but low spin in its heavier congeners. The optimized structural parameters also exhibit the expected trends,[19] with longer bonds in the high-spin states as a consequence of the occupation of M−Cl antibonding orbitals.

Table 1. Configurations Used To Model the Various States Referred to in the Text

MCl_6^{3-} state	configuration
$^6A_{1g}$	$t_{2g}^{3/0}e_g^{2/0}$
$^2T_{2g}$	$t_{2g}^{3/2}e_g^{0/0}$
$M_2Cl_9^{3-}$ state	configuration
BS	$a_1^{1/1}e^{2/2}e^{2/2}a_1^{0/0}e^{0/0}e^{0/0}$
$S = 0$ (HS)	$a_1'^{1/1}e'^{2/2}e'^{2/2}a_2''^{0/0}e''^{0/0}e''^{0/0}$
$S = 5$	$a_1'^{1/0}e'^{2/0}e''^{2/0}a_2''^{1/0}e''^{2/0}e'^{2/0}$
$S = 0$ (LS)	$a_1'^{1/1}e'^{2/2}e''^{2/2}a_2''^{0/0}e''^{0/0}e'^{0/0}$
$S = 1$	$a_1'^{1/0}e'^{2/2}e''^{2/2}a_2''^{1/0}e''^{0/0}e'^{0/0}$
$S = 1$b	$a_1'^{1/1}e'^{2/2}e''^{2/1}a_2''^{1/0}e''^{0/0}e'^{0/0}$
$S = 1$c	$a_1'^{1/1}e'^{2/2}e''^{2/0}a_2''^{1/1}e''^{0/0}e'^{0/0}$

Table 2. M−Cl Bond Lengths and Total Energies of the $^2T_{2g}$ and $^6A_{1g}$ States of MCl_6^{3-}

	$^2T_{2g}$		$^6A_{1g}$	
	M−Cl/Å	energy/eV	M−Cl/Å	energy/eV
$FeCl_6^{3-}$	2.347	−23.138	2.479	−24.053
$RuCl_6^{3-}$	2.455	−22.832	2.610	−21.521
$OsCl_6^{3-}$	2.501	−25.221	2.674	−23.552

Table 3. Energetic Parameters for MCl_6^{3-}, M = Fe, Ru, Os

	SPE(HS)/eV	SPE(LS)/eV	LFE/eV	ΔE(HS/LS)/eV
$FeCl_6^{3-}$	+3.46	+0.21	2.34	−0.91
$RuCl_6^{3-}$	+2.05	+0.11	3.25	+1.31
$OsCl_6^{3-}$	+1.84	+0.09	3.42	+1.67

Spin crossover is most often discussed in terms of two competing factors, the ligand-field splitting energy (LFE) and the spin-polarization energy (SPE), favoring low- and high-spin states, respectively. Quantitative estimates of the magnitude of these two factors can be obtained by defining reference states corresponding to the spin-*restricted* configurations $t_{2g}^5e_g^0$ and $t_{2g}^3e_g^2$, which differ from the low- and high-spin states defined previously only in the absence of the spin-polarization energy. The energetic difference between the two reference configurations gives a measure of the ligand-field energy, LFE. It should be noted that as defined here, the ligand-field energy is equal to twice the ligand-field splitting parameter, Δ, plus the difference in Coulomb repulsion in the two configurations. The SPE for each state can be evaluated by comparing the energies of the spin-unrestricted configuration and its reference counterpart. Values of LFE and SPE for the three complexes are collected in Table 3. It is clear from table that the dominant factor in establishing the high-spin ground state in the iron complex is the extremely high SPE associated with the presence of five unpaired electrons. In the larger metal ions, the increased interelectronic separation reduces the SPE in the high-spin state to such an extent that it cannot overcome the ligand-field splitting, and low-spin ground states prevail.

It is instructive to compare the SPE for the high- and low-spin states of the iron triad with those of the trivalent hexahalides

(9) (a) Musgrave, K. B.; Angove, H. C.; Burgess, B. K.; Hedman, B.; Hodgson, K. O. *J. Am. Chem. Soc.* **1998**, *120*, 5325. (b) Han, J.; Beck, K.; Ockwig, N.; Coucouvanis, D. *J. Am. Chem. Soc.* **1999**, *121*, 10448.
(10) Peters, J. W.; Stowell, M. H. B.; Soltis, S. M.; Finnegan, M. G.; Johnson, M. K.; Rees, D. C. *Biochemistry* **1997**, *36*, 1181.
(11) Shu, L.; Nesheim, J. C.; Kauffmann, K.; Munck, E.; Lipscomb, J.; Que, L., Jr. *Science* **1997**, *275*, 515.
(12) Rigga-Gelasco, P. J.; Shu, L.; Chen, S.; Burdi, D.; Huynh, B. H.; Que, L., Jr.; Stubbe, J. *J. Am. Chem. Soc.* **1998**, *120*, 849.
(13) Hwang, J.; Krebs, C.; Huynh, B. H.; Edmondson, D. E.; Theil, E. C.; Penner-Hahn, J. E. *Science* **2000**, *287*, 122.
(14) McGrady, J. E.; Stranger, R. *Inorg. Chem.* **1999**, *38*, 550.
(15) ADF 2.3.0, Theoretical Chemistry, Vrije Univeriteit, Amsterdam. (a) Baerends, E. J.; Ellis, D. E.; Ros, P. *Chem. Phys.* **1973**, *2*, 42. (b) te Velde, G.; Baerends, E. J. *J. Comput. Phys.* **1992**, *99*, 84.
(16) Parr, R. G.; Yang, W. *Density Functional Theory of Atoms and Molecules*; Oxford University Press: New York, 1989.
(17) Vosko, S. H.; Wilk, L.; Nusair, M. *Can. J. Phys.* **1980**, *58*, 1200.
(18) Versluis, L.; Ziegler, T. *J. Chem. Phys.* **1988**, *88*, 322.

Table 4. Metal−Metal Distances and Total Energies for the Broken-Symmetry (BS) and Associated States of $M_2Cl_9^{3-}$ [a]

	BS		$S = 0$ (HS)		$S = 5$		$S = 0$ (LS)		$S = 1$	
	M−M/Å	energy/eV	M−M/Å	energy/eV	M−M/Å	energy/eV	M−M/Å	energy/eV	M−M/Å	energy/eV
$Fe_2Cl_9^{3-}$	3.45	0.00	2.38	+6.14	3.45	+0.01	2.67	+1.59	3.07	+1.29
$Ru_2Cl_9^{3-}$	2.74	0.00	2.53	+6.00	3.65	+3.47	2.75	0.00	3.26	+0.48
$Os_2Cl_9^{3-}$	2.79	0.00	2.64	+6.27	3.73	+4.33	2.80	0.00	3.35	+0.67

[a] Energies are given relative to the minimum in the broken-symmetry-state curve.

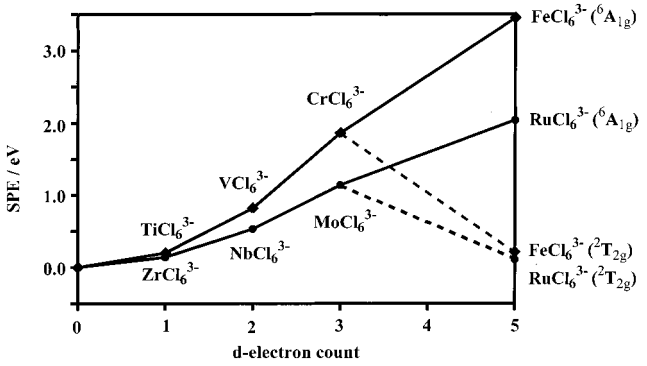

Figure 2. Calculated spin-polarization energy vs d electron configuration for MCl_6^{3-}. The plot for complexes of the third transition series is very similar to that for the second, so it is omitted for clarity.

of the chromium (d^3), vanadium (d^2), and titanium (d^1) triads calculated previously[1e] (Figure 2). The total SPE for a given state is, to a first approximation, proportional to the number of pairwise interactions between electrons of like spin,

$$\mathrm{SPE} \propto \frac{n(n-1)}{2}$$

where n is the number of unpaired electrons. The trends shown in Figure 2 are fully in accord with this simple expression, showing maxima for the d^3 and high-spin d^5 configurations. The values for the high-spin d^5 complexes are, however, somewhat lower than might have been anticipated on the basis of extrapolation of the d^1, d^2, and d^3 systems. This apparent anomally occurs because the fourth and fifth electrons enter the e_g orbital, which is much more extensively delocalized over the ligand array than its t_{2g} counterpart, thereby reducing the spin density on the metal. The most important point to note from Figure 2 is that the spin-polarization energy, which provides the driving force for the stabilization of high-spin states, is not linearly dependent on n but rather varies approximately as n^2. Thus, in the absence of significant changes in the ligand-field splitting parameter, the tendency to adopt a high-spin ground state increases dramatically as we approach the half-filled shell. While much of the above discussion could have been anticipated from a basic knowledge of undergraduate chemistry, the analysis of the various terms involved in the spin-crossover transition is critical to the understanding of the behavior of the bimetallic systems.

Bimetallic Systems. In previous papers we have used potential energy curves to investigate changes in the nature of metal−metal bonding as a function of the separation between the two centers. These ideas are extended here to incorporate the additional possibility that the component single ions can adopt either of the high- or low-spin configurations described in the previous section. We initially present a general description of the various states that can arise from coupling (strong and weak) between two single ions (high- or low-spin). The relative energies of these different states will then be examined for both $Fe_2Cl_9^{3-}$ and $Ru_2Cl_9^{3-}$ (the potential energy curves for the Os complex are very similar to those of its Ru analogue and so are not discussed explicitly).

Chart 1. Splitting of Metal-Based Orbitals in a Face-Shared Bioctahedron

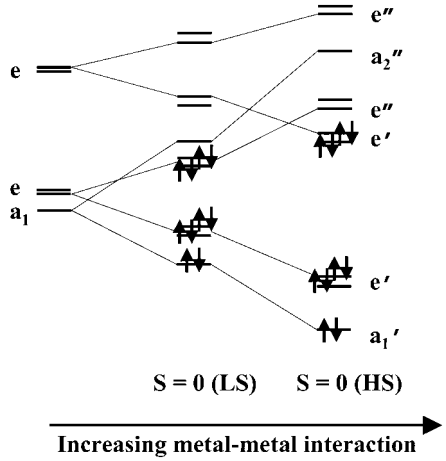

Strongly Coupled Limit. If all electrons are completely delocalized over both sides of the bioctahedron, then the metal-based orbitals split as shown in Chart 1. Where the interaction is moderately strong, the ground-state configuration corresponds to the occupation of the a_1', e', and e'' orbitals (all t_{2g}-based), giving a metal−metal bond order of 1. As the strength of the interaction increases, the bonding e' orbital of e_g parentage is stabilized and can, at least in principle, fall below the antibonding t_{2g}-based e'', giving a formal bond order of 5. The $a_1'^2e'^4e''^4$ configuration correlates with two single ions in the low-spin $^2T_{2g}$ ground state and so is denoted $S = 0$ (LS). The $a_1'^2e'^4e'^4$ configuration, in contrast, correlates with two high-spin $^6A_{1g}$ single ions states and is therefore denoted $S = 0$ (HS).

Weakly Coupled Limit. In the limit of weak antiferromagnetic coupling, metal-based electrons are not delocalized over both sides of the molecule but instead remain on a single metal center. The broken-symmetry methodology, developed by Noodleman and co-workers, provides a convenient mechanism for describing this weakly coupled limit by removing all symmetry elements connecting the two metal ions (corresponding, in this case, to a reduction in symmetry from D_{3h} to C_{3v}). As a result, the spin-α and spin-β electrons are permitted (but not forced) to localize on opposite sides of the molecule. Two limiting situations, corresponding to the coupling of high- and low-spin single-ion states, are summarized in Chart 2, where orbitals are now labeled according to the C_{3v} point group. The most significant point to note is that both the e' and e'' orbitals of D_{3h} symmetry transform as e in the C_{3v} point group, and as a result, both situations shown in Chart 2 correspond to the configuration $a_1^{1/1}e^{2/2}e^{2/2}$. This broken-symmetry configuration can, therefore, embrace both high- and low-spin single ions. Moreover, because the electrons have the freedom to delocalize over both centers, the broken symmetry state can also encompass both strongly and weakly coupled limits, as well as a range of intermediate cases.

Chart 2. Possible Electron Spin Distributions in Antiferromagnetically Coupled States of $M_2Cl_9^{3-}$, M = Fe, Ru, Os

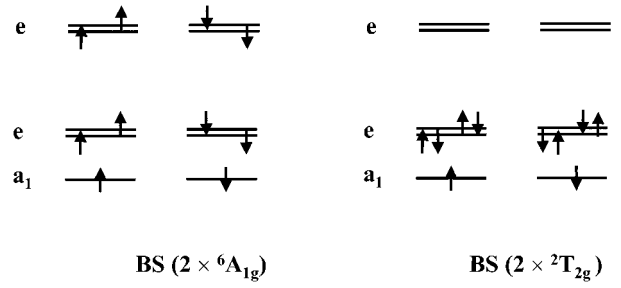

Chart 3. Electron Distributions in Nonsinglet States of $M_2Cl_9^{3-}$, M = Fe, Ru, Os

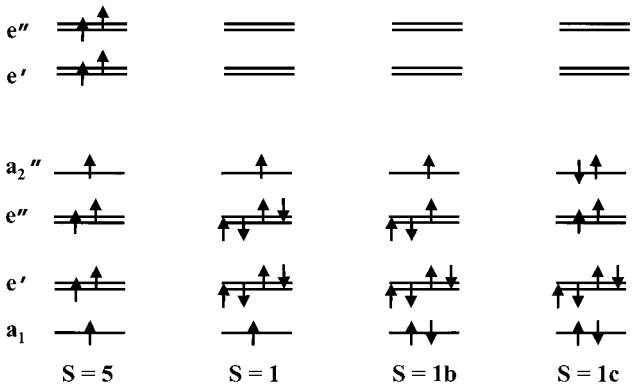

Ferromagnetic "Associated" States. Given the flexibility of the broken-symmetry state noted in the previous paragraph, it is not always straightforward to establish the precise nature of the metal−metal interaction at any given point on the potential energy curve. In previous publications, we have shown that the simplest way to do this is to consider the energetic proximity of high-spin "associated states", where the electrons are ferromagnetically coupled. For example, if the broken-symmetry state contains weakly coupled low-spin ($S = {}^1/_2$) single ions, then the associated ferromagnetically coupled state with $S = 1$ (Chart 3) will lie close to the broken-symmetry curve. Similarly, if the broken-symmetry state contains weakly coupled high-spin ($S = {}^5/_2$) ions, then the corresponding ferromagnetic associated state, with $S = 5$, will lie closest. In the following sections, we present broken-symmetry potential energy curves for both $Fe_2Cl_9^{3-}$ and $Ru_2Cl_9^{3-}$ and, by considering the proximity of the delocalized [$S = 0$ (HS) and $S = 0$ (LS)] and associated [$S = 1$ and $S = 5$] states, establish how the metal−metal interaction varies as a function of internuclear separation.

$Fe_2Cl_9^{3-}$. The potential energy curve for the broken-symmetry state of $Fe_2Cl_9^{3-}$ is shown as a bold line in Figure 3. At large Fe−Fe separations, the broken-symmetry state is almost coincident with $S = 5$, indicating that the two Fe^{III} ions are weakly coupled and are high-spin. Below 2.4 Å, however, the two curves diverge, the $S = 5$ state moving to higher energy, and the broken-symmetry curve instead converges with the $S = 0$ (LS) state. At short distances, therefore, the Fe^{III} centers have low-spin configurations and are linked by a single covalent Fe−Fe bond. The nature of the coupling between the metal ions therefore undergoes an abrupt transition at Fe−Fe = 2.4 Å, from weakly coupled *high-spin* to strongly coupled *low-spin* Fe^{III} centers. Both the $S = 1$ and $S = 0$ (HS) states (the latter is outside the energy range shown in Figure 3) lie well above the broken-symmetry curve at all points, confirming that there are no intermediate stages in this transition, corresponding either to weakly coupled low-spin [as in $S = 1$] or strongly coupled high-spin [as in $S = 0$(HS)] ions.

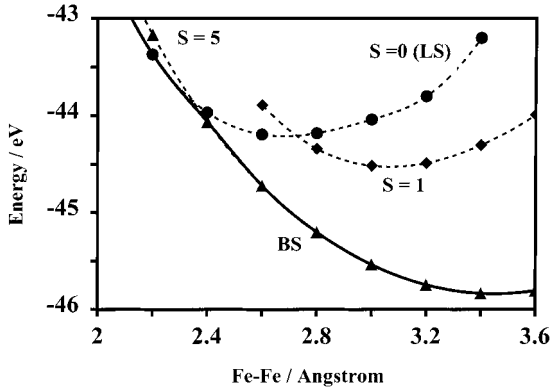

Figure 3. Potential energy curves for the broken-symmetry (bold) and associated states of $Fe_2Cl_9^{3-}$.

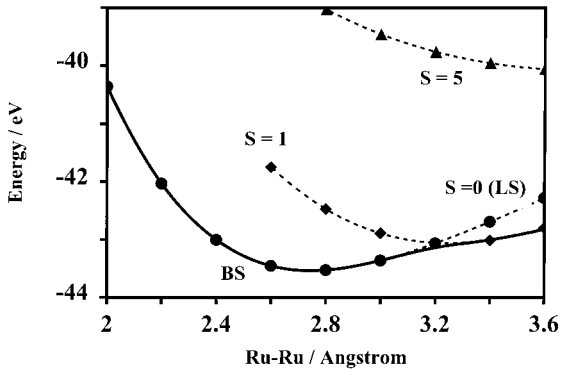

Figure 4. Potential energy curves for the broken-symmetry (bold) and associated states of $Ru_2Cl_9^{3-}$.

It should be noted at this point that the broken-symmetry state is not a pure singlet spin state and is contaminated with $M_s = 0$ components of higher lying nonsinglet states. The energy of the pure singlet state can, in principle, be extracted using spin projection techniques. However, in numerous related systems, we have shown that the potential energy curve for the spin-projected singlet closely follows that for the broken-symmetry state.[1c] Moreover, any significant deviation of the two curves can be traced to an inappropriate choice of S_{max}, the maximum spin state accessible by the system. In light of these comments, no attempt has been made to calculate spin-projected energies in this work.

$Ru_2Cl_9^{3-}$. The potential energy curve for the broken-symmetry state of $Ru_2Cl_9^{3-}$ is shown in bold in Figure 4. At short Ru−Ru separations, the nature of the metal−metal interaction is very similar to that observed in the iron analogue: the broken-symmetry curve is convergent with $S = 0$ (LS), indicating that the Ru^{III} ions are low-spin and are strongly coupled. The two curves remain coincident until Ru−Ru = 3.2 Å (compared to 2.4 Å in the iron analogue), and a minimum emerges at 2.74 Å, in excellent agreement with the value of 2.725 Å observed in $Cs_3Ru_2Cl_9$.[21] As in the iron system, the broken-symmetry curve deviates from $S = 0$ (LS) at longer

(19) Oshio, H.; Toriumi, K.; Maeda, Y.; Takashima, Y. *Inorg. Chem.* **1991**, *30*, 4252.

(20) (a) Noodleman, L.; Norman, J. G., Jr. *J. Chem. Phys.* **1979**, *70*, 4903. (b) Noodleman, L. *J. Chem. Phys.* **1981**, *74*, 5737.

(21) Darriet, J. *Rev. Chim. Miner.* **1981**, *18*, 27.

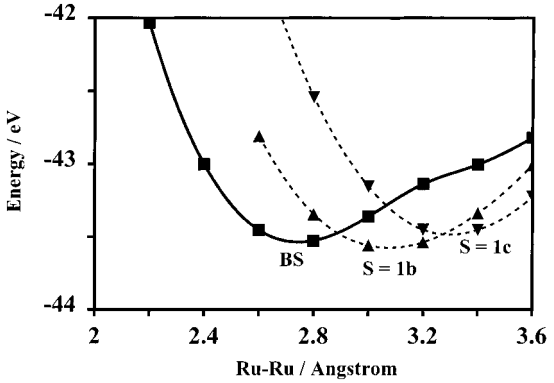

Figure 5. Potential energy curves for the broken-symmetry (bold) and triplet states of $Ru_2Cl_9^{3-}$.

separations, marking the point at which electrons begin to localize on opposite metal centers. However, instead of converging with the $S = 5$ associated state, as was the case for Fe, the broken-symmetry curve now lies close to $S = 1$, indicating that two low-spin, rather than high-spin, Ru^{III} centers are generated. The situation therefore contrasts dramatically with that in the iron analogue, where cleavage of the single Fe−Fe bond is accompanied by a switch from low- to high-spin single-ion configurations.

In the previous paragraph, we have simplified the discussion of the weakly coupled region by considering only states arising from vacancies in the nondegenerate (a_1) component of the t_{2g}-based manifold (BS and $S = 1$). In the absence of significant metal−metal bonding, however, the vacancy can also occur in one of the doubly degenerate (e) components. In a previous paper we have provided a detailed analysis of the states arising from coupling in d^1d^1 systems (which, from a symmetry perspective, is identical to the low-spin d^5d^5 case). On the basis of this previous work, we anticipate that two additional triplet states will enter the valence region, corresponding to (i) a single vacancy in each of the e and a_1 orbitals ($S = 1$b) and (ii) two vacancies in the e manifold ($S = 1$c) (see Chart 3). Potential energy curves for these additional states are plotted in Figure 5, along with the BS curve (other states are removed for clarity). At separations greater than 2.9 Å, the triplet $S = 1$b falls below $S = 0$ (LS), while beyond 3.3 Å, $S = 1$c is most stable. The minima in the $S = 1$b state at 3.07 Å is, in fact, more stable than the broken-symmetry minimum at 2.74 Å, an observation that is inconsistent with the observed Ru−Ru separation of 2.725(1) Å. However, the two minima are separated by only 2 kJ mol^{-1} and, moreover, their relative energies are strongly affected by changes in the computational method (the inclusion of quasi-relativistic effects, for example, stabilizes $S = 0$ (LS) relative to $S = 1$b). Given the very small separation of these two states, it is not possible to identify with certainty the true ground state in $Ru_2Cl_9^{3-}$. What is clear, however, is that the potential energy surface is very flat, and the Ru−Ru separation may be highly susceptible to cation size, just as the Mo−Mo separation is in $Mo_2Cl_9^{3-}$.[1c] This prediction cannot, however, be verified experimentally at this time, as only the cesium salt of $Ru_2Cl_9^{3-}$ has been characterized crystallographically.

Discussion

The abrupt change in nature of the broken-symmetry state at 2.4 Å in the iron complex indicates that the conceptually distinct processes of metal−metal bond formation and spin crossover are in fact intimately linked. Their mutual interdependence can be traced to the pivotal role of the single-ion SPE, which favors both the retention of high-spin single-ion states and the retention of localized electron spin distributions in bimetallic systems. Covalent bond formation reduces the spin density on the metal center and therefore causes a shift toward low-spin single-ion states and also toward delocalized electron spin distributions. In this context, the only difference between the two phenomena discussed in this paper (spin crossover and metal−metal bonding) is the partner in the covalent bond: an array of ligand atoms in the case of former; another metal atom in the latter. Thus, any factor that increases the spin-polarization energy will necessarily favor high-spin single ion configurations and, at the same time, enforce weak coupling between the centers. A corollary to this statement is that high-spin single-ion configurations and strong metal−metal bonding are mutually incompatible. In the iron system studied in this paper, the point at which the broken-symmetry state switches from antiferromagnetically coupled high-spin to strongly coupled low-spin is sufficiently far, in energetic terms, above the global minimum not to have any impact on the ground-state properties of the system. This may not, however, always be the case, and it is instructive at this point to recall that reduction of biological iron−sulfur cubanes induces substantial changes in Fe−Fe distances.[9] Reduction of Fe^{III} (d^5) to Fe^{II} (d^6) involves a large reduction in the SPE (see Figure 2), and so the titration of electrons into iron cubane clusters should favor both the adoption of low-spin states and the formation of metal−metal bonds. The results reported in this paper suggest that the two processes may be intimately linked.

Acknowledgment. The Australian Research Council and the Engineering and Physical Sciences Research Council (U.K.) are gratefully acknowledged for financial support. T.L. also acknowledges the latter for an overseas scholarship.

IC0004737